Check for updates

Received: 2 October 2023 | Revised: 17 October 2023 | Accepted: 20 October 2023

DOI: 10.1002/jcu.23603

RESEARCH ARTICLE

WILEY

Correlations between vegetative autonomic function and specific left atrial functions in healthy adults: Insights from the three-dimensional speckle-tracking echocardiographic MAGYAR-Healthy Study

Attila Nemes MD, PhD, DSc, FESC[1] | Árpád Kormányos MD, PhD[1] | Andrea Orosz MD, PhD[2] | Nóra Ambrus MD, PhD[1] | Tamás T. Várkonyi MD, PhD[1] | Csaba Lengyel MD, PhD[1]

[1]Department of Medicine, Albert Szent-Györgyi Medical School, University of Szeged, Szeged, Hungary

[2]Department of Pharmacology and Pharmacotherapy, Albert Szent-Györgyi Medical School, University of Szeged, Szeged, Hungary

Correspondence
Attila Nemes, Department of Medicine, Albert Szent-Györgyi Medical School, University of Szeged, Semmelweis Street 8, P.O. Box 427, Szeged H-6725, Hungary.
Email: nemes.attila@med.u-szeged.hu

Abstract

Introduction: The functioning of the left atrium (LA) is partly controlled by the neural system. It was purposed to evaluate correlations between the result of Ewing's 5 standard cardiovascular reflex tests (SCRTs) characterizing autonomic function and LA volumetric and functional features as assessed by three-dimensional speckle-tracking echocardiography (3DSTE) in healthy individuals.

Materials and Methods: The current study comprised 18 healthy volunteers being in sinus rhythm (mean age: 35 ± 12 years, 10 men). Measurement of blood pressure, ECG, 5 SCRTs, two-dimensional Doppler echocardiography and 3DSTE were performed. These parameters were in normal ranges in all cases.

Results: From LA volumetric parameters, only systolic total atrial emptying fraction ($r = 0.559$, $p = 0.037$) and early diastolic passive atrial emptying fraction ($r = 0.539$, $p = 0.047$) correlated with systolic blood pressure response to standing representing sympathetic autonomic function. From LA strains, peak mean segmental LA radial strain (RS) ($r = -0.532$, $p = 0.050$), global and mean segmental LA circumferential strain (CS) ($r = 0.662$, $p = 0.010$ and $r = 0.635$, $p = 0.015$, respectively) representing systolic LA function correlated with Valsalva ratio representing parasympathetic autonomic function. Global LA-RS ($r = -0.713$, $p = 0.040$) and LA-CS ($r = 0.657$, $p = 0.011$) and mean segmental LA-CS ($r = 0.723$, $p = 0.003$) at atrial contraction representing end-diastolic atrial contraction showed correlations with Valsalva ratio, as well. Peak global and mean segmental LA-CS ($r = 0.532$, $p = 0.050$ and $r = 0.530$, $p = 0.050$) and the same strains at atrial contraction ($r = 0.704$, $p = 0.005$ and $r = 0.690$, $p = 0.006$) representing systolic function and end-diastolic atrial contraction correlated with systolic blood pressure response to standing representing both parasympathetic and sympathetic autonomic functions.

Conclusions: Significant correlations between features of vegetative autonomic function represented by Ewing's 5 SCRTs and specific LA functions represented by 3DSTE-derived LA volume-based functional properties and strains could be demonstrated in healthy adults.

 © 2023 Wiley Periodicals LLC.

KEYWORDS
autonomic, correlation, echocardiography, left atrial, speckle-tracking, three-dimensional

1 | INTRODUCTION

Evaluation of cardiovascular functions in healthy humans using modern non-invasive methods allows detailed analysis of physiological relationships. As a result, the factors playing a role in the normal volumetric and functional properties of atria and ventricles could be identified. The left atrium (LA) has a central role in regulating normal blood flow from the pulmonary veins to the left ventricle (LV) before valvular regurgitations or stenoses develop.[1–4] LA is a cardiac chamber with a special behavior during the cardiac cycle having a reservoir role in systole, working as a conduit in early diastole and having an active contraction in later diastole.[1–4]

The heart is under essential neural regulation via the cardiac plexus including both sympathetic and parasympathetic systems.[5–7] Preganglionic fibers from left and right vagal nerves contribute to the parasympathetic function reaching the ganglia in the cardiac plexus and the atrial walls and are responsible for coronary vasoconstriction and for reducing heart rate and cardiac contraction. The sympathetic innervation is different with the preganglionic fibers branching from the upper thoracic spinal cord, ganglionic connections in the lower cervical and upper thoracic ganglia and postganglional fibers reaching the cardiac plexus and by having opposite effects on heart rate and cardiac contraction.[5–7] The Ewing's standard cardiovascular reflex test (SCRT) is a relatively easy-to-implement way to feature sympathetic and parasympathetic functions.[5] However, the exact relationship between autonomic function and detailed LA functions has not been examined.

Novel cardiovascular imaging techniques are capable for detailed volumetric and functional examination of cardiac chambers. Three-dimensional speckle-tracking echocardiography (3DSTE) is considered to be one of the most up-to-date non-invasive imaging methods with volumetric and strain analyses representing wall contractility features.[8–11] Until now, the relationship between LA functions and vegetative autonomic function was not fully examined in real-life clinical settings in healthy circumstances, therefore the present study purposed to analyze correlations between the result of Ewing's SCRTs characterizing autonomic function and LA volumetric and functional features as assessed by 3DSTE in healthy adults.

2 | METHODS

2.1 | Study population

The study comprised 18 healthy volunteers being in sinus rhythm (mean age: 35 ± 12 years, 10 men). None of them were smoker or obese. Electrocardiography (ECG), antropometric, laboratory and blood pressure measurements, 5 Ewing's SCRTs, two-dimensional Doppler echocardiography (2DDE) and 3DSTE were performed in all subjects, and all parameters were in normal ranges. None of the subjects had any known disorder, pathologic state or cardiovascular risk factor. There were no other factors present, which could theoretically affect the results. The present study is the part of the MAGYAR-Healthy Study (Motion Analysis of the heart and Great vessels bY three-dimensionAl speckle-tRacking echocardiography in Healthy subjects), which were organized in our department. Among a number of objectives, our aim was to examine physiologic relationships between different parameters in healthy adult subjects ("magyar" means "Hungarian" in Hungarian language). Institutional and Regional Human Biomedical Research Committee of University of Szeged, Hungary (No: 71/2011, prolonged February 20/2023) approved the study, which complied with the Declaration of Helsinki. All participants gave an informed consent.

2.2 | Two-dimensional Doppler echocardiography

Conventional 2DDE was performed in all subjects by a Toshiba Artida™ echocardiographic tool (Toshiba Medical Systems, Tokyo, Japan) attached to a 1–5 MHz PST-30SBT phased-array transducer. Chamber quantifications and valvular assessments were performed in accordance with recent guidelines. Parasternal LA diameter and standard LV dimensions were measured, LV volumes and ejection fraction were determined by the Simpson's method. Doppler echocardiography was used to exclude significant valvular regurgitations or stenoses.[12]

2.3 | Three-dimensional speckle-tracking echocardiography

3DSTE was performed according to recent practices as described earlier in more detail.[13,14] Shortly, using the same Toshiba Artida™ echocardiography equipment (Toshiba Medical Systems, Tokyo, Japan), the transducer was replaced to a PST-25SX matrix 1–4 MHz phased-array transducer for 3D echocardiographic data acquisitions.[8–11] The subject had to be in sinus rhythm, the acquisitions were made in a breath-hold just before the autonomic neuropathy tests. Following optimizations of gain and size, a 3D echocardiographic dataset was acquired, which contained 6 wedge-shaped "subvolumes" from the apical window. From all subjects 3–4 datasets were acquired. From these subvolumes, the software was able to create a 3D "full-volume" dataset by attaching echocardiographic subvolumes to each other according to successive beats; measurements could be performed on these datasets using a special software (3D Wall Motion Tracking software version 2.7, Toshiba Medical Systems, Tokyo, Japan). Following an automatic display, data were presented in multiple plane views including apical two- (AP2CH) and four-chamber (AP4CH) longitudinal views and short-axis views at basal, midatrial and superior

10970096, 0, Downloaded from https://onlinelibrary.wiley.com/doi/10.1002/jcu.23603 by University Of Szeged, Wiley Online Library on [26/11/2023]. See the Terms and Conditions (https://onlinelibrary.wiley.com/terms-and-conditions) on Wiley Online Library for rules of use; OA articles are governed by the applicable Creative Commons License

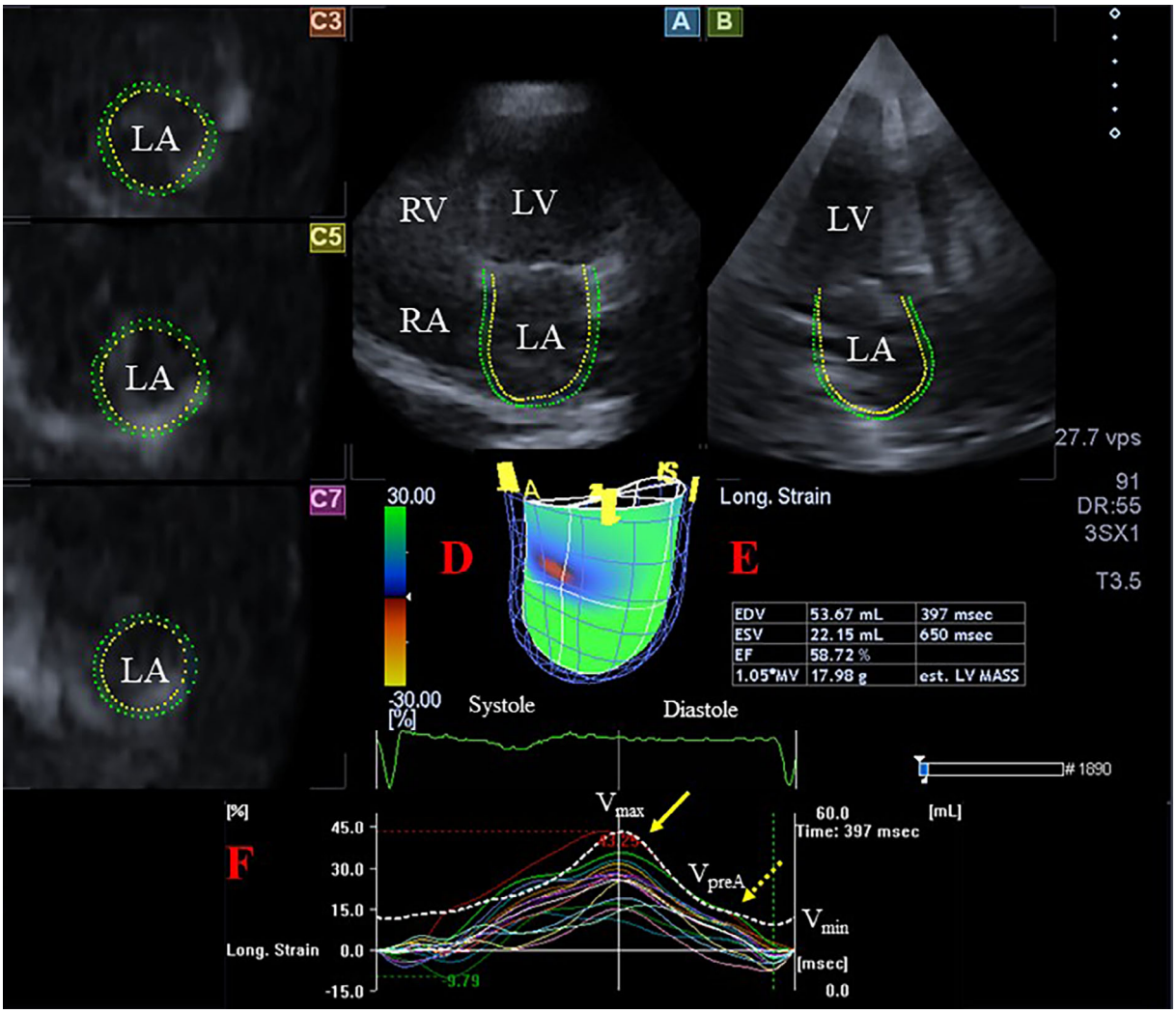

FIGURE 1 Analysis of the left atrium (LA) by three-dimensional speckle-tracking echocardiography: apical four-chamber (A) and two-chamber (B) longitudinal views and 3 short-axis views (C3, C5, C7) at different LA levels are presented in a healthy man. Three-dimensional cast of the LA (red D) and segmental LA strains (E) are demonstrated together with LA volumetric data (F). Yellow arrow represents peak LA strains, while dashed yellow arrow represents LA strains at atrial contraction. EDV, end-diastolic volume; EF, ejection fraction; ESV, end-systolic volume; LA, left atrium; LV, left ventricle; RA, right atrium; RV, right ventricle.

regions. For the measurements, reference points were set on the edge of mitral annulus—septum, then markers were placed in a counterclockwise direction around the LA toward the edge of mitral annulus—lateral wall in AP4CH and AP2CH views. LA appendage and pulmonary veins were excluded from the evaluations. Then, automatic tracking of 3D wall motion was performed through the heart cycle creating a 3DSTE-based virtual model of the LA (Figure 1).[8–11]

2.4 | 3DSTE-derived LA volumetric assessments

Using the 3DSTE-derived LA cast, the following LA volumes were measured[13]:

1. End-systolic maximum LA volume (LA volume is the largest just before mitral valve opening, V_{max}),
2. Diastolic LA volume before atrial contraction measured at the last frame before mitral valve reopening or at the time of P wave on ECG (V_{preA}).
3. End-diastolic minimum LA volume (LA volume is the lowest just before mitral valve closure, V_{min}).

The following LA volume-based functional properties were calculated from LA volumes.[13]

Systolic reservoir function:

1. Total Atrial Stroke Volume (TASV): $V_{max} - V_{min}$.
2. Total Atrial Emptying Fraction (TAEF): $TASV/V_{max} \times 100$.

Early diastolic conduit function:

1. Passive Atrial Stroke Volume (PASV): $V_{max} - V_{preA}$.
2. Passive Atrial Emptying Fraction (PAEF): $PASV/V_{max} \times 100$.

10970096, 0, Downloaded from https://onlinelibrary.wiley.com/doi/10.1002/jcu.23603 by University Of Szeged, Wiley Online Library on [26/11/2023]. See the Terms and Conditions (https://onlinelibrary.wiley.com/terms-and-conditions) on Wiley Online Library for rules of use; OA articles are governed by the applicable Creative Commons License

Late diastolic active contraction:

1. Active Atrial Stroke Volume (AASV): $V_{preA} - V_{min}$.
2. Active Atrial Emptying Fraction (AAEF): $AASV/V_{preA} \times 100$.

2.5 | 3DSTE-derived LA strain measurements

The following global and mean segmental LA strains were automatically measured by the software at the same time using the same 3DSTE-derived LA cast[14]:

1. Longitudinal strain representing lengthening and shortening of LA segments (LS)
2. Circumferential strain representing widening and narrowing of LA segments (CS)
3. Radial strain representing thickening and thinning of LA segments (RS)
4. Area strain as a combination of LS and CS
5. 3D strain as a combination of RS, LS and CS

Following 3DSTE-derived detection of LA strain curves, they proved to be double peaked. The first peak represented systolic LA reservoir function, while the second peak represented end-diastolic atrial contraction (booster bump function).

2.6 | Autonomic function

Autonomic function was assessed by means of 5 Ewing's SCRTs.[5,15,16]

For predominantly characterizing parasympathetic function:

1. In case of heart rate response to deep breathing (HRRDB), the subject was asked to have a deep breath at the rate of six breaths per minute (5 s in and 5 s out). The findings were expressed as the difference between the measured maximum and minimum heart rates (beats/min) during the six breathing cycles (normal value: ≥15 bpm, abnormal value: ≤10 bpm).
2. In case of calculation of Valsalva ratio (VR), the subject was asked to blow into a mouthpiece connected to a modified manometer and holding it at a pressure of 40 mmHg for 15 s under a continuous recording of ECG. The Valsalva ratio was calculated as the ratio of the longest R-R interval after the procedure to the shortest R-R interval during the maneuver (normal value: ≥1.21, abnormal value: ≤1.10).
3. In case of calculation of 30/15 ratio, the subject was asked to remain in the supine position while continuous ECG recording was done, then the subjects was instructed to stand up without interrupting the recording. The 30/15 ratio was calculated as the ratio of the longest R-R interval (at around the 30th beat) to the shortest R-R interval (at around the 15th beat) following standing up (normal value: ≥1.03, abnormal value: ≤1.00).

For predominantly characterizing sympathetic function:

1. In case of sustained handgrip test (SHT), the subject was instructed to have a sustained hand grip. The maximum voluntary contraction was-first determined, then maintained at 30% of that maximum for as long as possible up to 5 min. Blood pressure (BP) was measured 3 times before and at one-minute intervals. The findings were demonstrated as the difference between the highest diastolic BP during handgrip exercise and the mean of the three diastolic BP readings before handgrip began (normal value: ≥16 mmHg, abnormal value: ≤10 mmHg).
2. In case of systolic blood pressure response to standing (SBPRS), BP was measured in lying position and following standing up. The postural BP fall was defined as the difference between systolic BP after 10 min in the supine position and systolic BPs at the 1st, 5th, and 10th minutes after standing up. The largest difference from the systolic BP in lying was evaluated as the BP response to standing (normal value: ≤10 mmHg, abnormal value: ≥30 mmHg).

To express the severity of the lesion of the autonomic function, autonomic neuropathy score (ANS) was calculated. In every above mentioned test, normal values were scored 0, borderline values 1 and abnormal values 2. The sum of the scores gave the total ANS (range 0–10). A score was considered to be normal if 0–1, borderline if 2–3 and abnormal if >3.[5,15,16]

2.7 | Statistical analysis

Continuous and categorical variables were presented in the following formats: mean ± standard deviation format or number and percentage format. The selected significance level was p less than 0.05. Pearson's correlation coefficients were calculated for numerical correlations. Confounders were examined by multivariable regression analysis. SPSS software (SPSS Inc, Chicago, IL, USA) was used for statistical calculations.

3 | RESULTS

3.1 | Baseline characteristics

Weight (65.2 ± 2.2 kg), height (165.2 ± 4.9 cm), body mass index (23.9 ± 1.0 kg/m^2), systolic (118.2 ± 3.8 mm Hg) and diastolic blood pressure (118.2 ± 3.8 mm mm Hg) and heart rate (71.2 ± 2.3 1/s) were in normal ranges in all subjects. From laboratory results, HbA1c (3.5 ± 0.7%), low density lipoprotein (65.2 ± 21.3 mg/dL) levels and estimated glomerular filtration rate (88.2 ± 5.1 mL/min/1.73 m^2) proved to be normal as well.

3.2 | Standard cardiovascular reflex tests

HRRDB (22.1 ± 7.0 bpm), VR (1.87 ± 0.19), 30:15 ratio (1.44 ± 0.23), SHT (20.5 ± 6.59 mmHg), SBPRS (4.29 ± 6.41 mmHg) and ANS (0.57 ± 1.24) were in normal ranges.

10970096, 0, Downloaded from https://onlinelibrary.wiley.com/doi/10.1002/jcu.23603 by University Of Szeged, Wiley Online Library on [26/11/2023]. See the Terms and Conditions (https://onlinelibrary.wiley.com/terms-and-conditions) on Wiley Online Library for rules of use; OA articles are governed by the applicable Creative Commons License

3.3 | Two-dimensional echocardiography

LV end-diastolic and end-systolic diameters (48.8 ± 2.5 mm and 33.3 ± 3.7 mm, respectively) and volumes (107.9 ± 17.5 mL and 39.2 ± 8.6 mL, respectively), thickness of the interventricular septum and LV posterior wall (8.9 ± 1.1 mm and 8.8 ± 0.7 mm, respectively), LV ejection fraction (64.0 ± 2.9%) and LA diameter in the parasternal long-axis view (39.5 ± 2.7 mm) were measured. Mean transmitral E and A inflow velocities and their ratio proved to be 79.1 ± 13.2 cm/s, 59.8 ± 12.5 cm/s, and 1.37 ± 0.31, respectively. None of the subjects showed ≥grade 1 valvular regurgitation or significant valvular stenosis.

3.4 | Three-dimensional speckle-tracking echocardiography

3DSTE-derived V_{max} (40.4 ± 14.1 mL), V_{preA} (28.9 ± 12.8 mL), V_{min} (18.8 ± 6.0 mL), TASV (21.7 ± 12.2 mL), PASV (11.5 ± 6.5 mL), AASV (10.2 ± 9.9 mL), TAEF (50.6 ± 17.4%), PAEF (28.9 ± 15.4%), and AAEF (30.5 ± 16.4%) were in normal ranges, as well, together with peak global and mean segmental LA-RS (−14.3 ± 9.7% and −19.7 ± 8.5%, respectively), LA-CS (38.4 ± 19.9% and 42.7 ± 19.4%, respectively) and LA-LS (25.1 ± 9.5% and 28.1 ± 9.3%, respectively) and global and mean segmental LA-RS (−5.7 ± 5.3% and − 8.5 ± 4.5%, respectively), LA-CS (17.1 ± 11.0% and 17.7 ± 9.0%, respectively) and LA-LS (7.0 ± 5.6% and 9.2 ± 3.7%, respectively) at atrial contraction.

3.5 | Correlations and linear regression analysis

Pearson's correlation coefficients between SCRTs and LA volumetric parameters and strains are presented in Tables 1 and 2. From LA volumetric parameters, only systolic TAEF and early diastolic PAEF correlated with the SBPRS representing sympathetic autonomic function. None of the other LA volumes and stroke volumes showed correlations with SCRTs. From LA strains, peak mean segmental LA-RS, global and mean segmental LA-CS representing systolic LA function correlated with VR representing parasympathetic autonomic function. Global LA-RS and LA-CS and mean segmental LA-CS at atrial contraction representing end-diastolic atrial contraction correlated with VR, as well. Peak global and mean segmental LA-CS and the same strains at atrial contraction representing systolic function and end-diastolic atrial contraction correlated with the SBPRS representing both parasympathetic and sympathetic autonomic functions.

Several confounders including age [Odd ratio (OR) = 0.99, 95% confidence interval (CI): 0.99–1.01], gender [OR = 1.05, 95% CI: 0.97–1.10], body mass index [OR = 1.15, 95% CI: 0.94–1.35], heart rate [OR = 0.95, 95% CI: 0.91–1.00] and systolic [OR = 0.97, 95% CI:

TABLE 1 Pearson's correlation coefficients between left atrial volumes and volumes-based functional properties and standard cardiovascular reflex tests in healthy adults.

	Parasympathetic function			Sympathetic function		
	Heart rate response to deep breathing	Valsalva ratio	30/15 ratio	Sustained handgrip test	Systolic blood pressure response to standing	Autonomic neuropathy score
Left atrial volumes						
V_{max}	−0.185 ($p = 0.527$)	0.165 ($p = 0.573$)	−0.336 ($p = 0.240$)	−0.268 ($p = 0.353$)	0.282 ($p = 0.329$)	0.505 ($p = 0.066$)
V_{preA}	−0.106 ($p = 0.719$)	−0.130 ($p = 0.659$)	−0.481 ($p = 0.081$)	−0.092 ($p = 0.753$)	−0.131 ($p = 0.656$)	0.291 ($p = 0.314$)
V_{min}	−0.194 ($p = 507$)	−0.385 ($p = 0.175$)	−0.262 ($p = 0.366$)	−0.097 ($p = 0.742$)	−0.261 ($p = 0.367$)	0.462 ($p = 0.096$)
Left atrial stroke volumes						
TASV	−0.154 ($p = 0.599$)	0.371 ($p = 0.191$)	−0.279 ($p = 0.334$)	−0.407 ($p = 0.149$)	0.323 ($p = 0.260$)	0.339 ($p = 0.235$)
PASV	−0.137 ($p = 0.641$)	0.213 ($p = 0.464$)	−0.015 ($p = 0.958$)	−0.333 ($p = 0.245$)	0.467 ($p = 0.092$)	0.404 ($p = 0.152$)
AASV	−0.148 ($p = 0.615$)	0.147 ($p = 0.615$)	−0.411 ($p = 0.144$)	−0.420 ($p = 0.135$)	0.236 ($p = 0.416$)	0.339 ($p = 0.235$)
Left atrial emptying fractions						
TAEF	0.026 ($p = 0.929$)	0.495 ($p = 0.072$)	−0.165 ($p = 0.573$)	−0.211 ($p = 0.469$)	**0.559 ($p = 0.037$)**	0.052 ($p = 0.860$)
PAEF	−0.081 ($p = 0.782$)	0.407 ($p = 0.149$)	0.235 ($p = 0.418$)	−0.209 ($p = 0.473$)	**0.539 ($p = 0.047$)**	0.113 ($p = 0.700$)
AAEF	−0.075 ($p = 0.799$)	0.380 ($p = 0.180$)	−0.336 ($p = 0.240$)	−0.385 ($p = 0.174$)	0.371 ($p = 0.191$)	0.217 ($p = 0.456$)

Note: Bold values are significant.

10970096, 0, Downloaded from https://onlinelibrary.wiley.com/doi/10.1002/jcu.23603 by University Of Szeged, Wiley Online Library on [26/11/2023]. See the Terms and Conditions (https://onlinelibrary.wiley.com/terms-and-conditions) on Wiley Online Library for rules of use; OA articles are governed by the applicable Creative Commons License

TABLE 2 Pearson's correlation coefficients between left atrial strains and standard cardiovascular reflex tests in healthy adults.

	Parasympathetic function			Sympathetic function		
	Heart rate response to deep breathing	Valsalva ratio	30/15 ratio	Sustained handgrip test	Systolic blood pressure response to standing	Autonomic neuropathy score
Peak left atrial strains						
Global LA-RS	0.165 ($p = 0.572$)	−0.512 ($p = 0.061$)	0.174 ($p = 0.553$)	0.112 ($p = 0.703$)	−0.131 ($p = 0.656$)	−0.156 ($p = 0.594$)
Mean segmental LA-RS	0.221 ($p = 0.449$)	**−0.532 ($p = 0.050$)**	0.277 ($p = 0.337$)	0.064 ($p = 0.828$)	−0.009 ($p = 0.975$)	−0.070 ($p = 0.811$)
Global LA-CS	0.046 ($p = 0.875$)	**0.662 ($p = 0.010$)**	−0.165 ($p = 0.573$)	−0.183 ($p = 0.532$)	**0.532 ($p = 0.050$)**	0.076 ($p = 0.795$)
Mean segmental LA-CS	0.040 ($p = 0.893$)	**0.635 ($p = 0.015$)**	−0.138 ($p = 0.637$)	−0.194 ($p = 0.507$)	**0.530 ($p = 0.050$)**	0.248 ($p = 0.393$)
Global LA-LS	0.139 ($p = 0.636$)	0.398 ($p = 0.159$)	−0.191 ($p = 0.513$)	−0.317 ($p = 0.270$)	0.078 ($p = 0.791$)	0.028 ($p = 0.926$)
Mean segmental LA-LS	0.126 ($p = 0.669$)	0.407 ($p = 0.149$)	−0.147 ($p = 0.615$)	−0.293 ($p = 0.310$)	0.055 ($p = 0.852$)	−0.009 ($p = 0.975$)
Left atrial strains at atrial contraction						
Global LA-RS	0.267 ($p = 0.356$)	**−0.715 ($p = 0.004$)**	−0.029 ($p = 0.923$)	0.264 ($p = 0.361$)	−0.468 ($p = 0.091$)	−0.242 ($p = 0.405$)
Mean segmental LA-RS	0.112 ($p = 0.702$)	−0.367 ($p = 0.197$)	0.059 ($p = 0.840$)	−0.097 ($p = 0.742$)	−0.099 ($p = 0.737$)	0.003 ($p = 0.992$)
Global LA-CS	−0.126 ($p = 0.669$)	**0.657 ($p = 0.011$)**	0.116 ($p = 0.692$)	−0.282 ($p = 0.329$)	**0.704 ($p = 0.005$)**	0.297 ($p = 0.303$)
Mean segmental LA-CS	−0.156 ($p = 0.593$)	**0.723 ($p = 0.003$)**	0.116 ($p = 0.692$)	−0.383 ($p = 0.177$)	**0.690 ($p = 0.006$)**	0.028 ($p = 0.926$)
Global LA-LS	0.066 ($p = 0.822$)	0.002 ($p = 0.994$)	0.405 ($p = 0.151$)	0.009 ($p = 0.976$)	−0.117 ($p = 0.690$)	0.119 ($p = 0.684$)
Mean segmental LA-LS	0.109 ($p = 0.710$)	0.273 ($p = 0.345$)	0.205 ($p = 0.482$)	−0.205 ($p = 0.482$)	0.177 ($p = 0.545$)	0.230 ($p = 0.429$)

Note: Bold values are significant.

0.93–1.02] and diastolic [OR = 0.99, 95% CI: 0.94–1.05] blood pressures were analyzed, but none of these parameters were a significant confounder during multivariable regression analysis.

4 | DISCUSSION

The present investigation is the first, to the knowledge of the authors, which aimed to examine direct associations between LA volumetric and functional properties and autonomic function in real-life settings using clinical methods in healthy adult volunteers. In systole, LA works like a reservoir, when the pulmonary veins fill the LA, which could be characterized by LA volumes and volume-based functional properties (V_{max}, TASV and TAEF) and peak LA strains as assessed at the same time by 3DSTE. According to the results of this study, VR representing predominantly the parasympathetic autonomic function showed correlations only with LA-RS and LA-CS from LA strains in healthy adult subjects. Higher parasympathetic function (represented by higher VR) correlated with LA thickening in radial direction (represented by LA-RS) and widening in circumferential direction (represented by LA-CS). Moreover, higher SBPRS correlated with higher TAEF and LA-CS as well, meaning associations between lower sympathetic function and higher LA circumferential widening and enhanced LA emptying. In early diastole, LA works like a conduit, the mitral valve opens and the LA empties. 3DSTE-derived V_{preA}, PASV and PAEF are capable of featuring this function, from which only PAEF correlated with SBPRS. Similarly to what could be seen in systole, lower sympathetic function was associated with enhanced LA emptying. In late diastole, LA actively contracts and has a booster pump function, which could be characterized by V_{min}, AASV and AAEF and LA strains at atrial contraction. Correlations

10970096, 0, Downloaded from https://onlinelibrary.wiley.com/doi/10.1002/jcu.23603 by University Of Szeged, Wiley Online Library on [26/11/2023]. See the Terms and Conditions (https://onlinelibrary.wiley.com/terms-and-conditions) on Wiley Online Library for rules of use; OA articles are governed by the applicable Creative Commons License

between VR and LA-RS and LA-CS and SBPRS with LA-CS were similar as in systole. The ANS did not correlate with any LA volumetric parameters and strains.

Pulmonary veins, LA, mitral valve, LV, aorta and the right heart show a significant interplay ruled by neural control. All these chambers and vessels have effects on each other as well even in healthy circumstances before any other (risk) factors play any role. In clinical circumstances, it is difficult to examine the effects on autonomic function, the relatively simple Ewing's SCRTs could help in this.[5] In a recent study, increased parasympathetic function was demonstrated to be associated with a decrease in LV apical rotation and LV twist. No relationship was found between Ewing's SCRTs mainly characterizing sympathetic autonomic function and LV rotational parameters.[17] Moreover, correlations existed between aortic distensibility and autonomic function, as well.[18]

Results of the present study are important regarding that the parasympathetic nervous system is thought to contribute significantly to focal atrial fibrillation (AF).[19] In AF patients during the ablation of left posterior wall ganglia vagal responses due to the relationship of the LA with these ganglionated plexi was already encountered.[20] The results may draw attention to the fact that in clinical conditions complicated by early disturbances of autonomic function (e.g., diabetes mellitus), the relationships described above may be even more complicated or even lost. Therefore, further studies are needed in certain pathological states. In the present study correlations could be shown between features of vegetative autonomic function and specific LA functions in everyday healthy subjects using a routine image technique 3DSTE providing (patho)physiologic insights into their complex relationship. However, further studies are warranted to confirm our results in a larger healthy population with other methods.

4.1 | Limitations

There were several important limitations:

1. A relatively small number of healthy individuals were enrolled in the present study.
2. The present study demonstrates only a simplified relationship (correlations) between LA volumes and function and vegetative autonomic function. Both methods (3DSTE and Ewing's test) are only simplified approaches for the evaluation of LA and vegetative autonomic functions.
3. Theoretically different results could come out in different autonomic tone conditions even in healthy circumstances or in different pathological states. However, this would a topic of further investigations.
4. 3DSTE has a limited image quality due to technical reasons (large transducer, limited number of chrystals, low spatial and temporal resolution).[8–11]
5. Although all cardiac chambers could be analyzed by 3DSTE, only volumetric and strain analysis of LA was performed.
6. It was not purposed to validate 3DSTE-derived LA volumetric and functional properties.
7. LA strains are affected by several factors. Although healthy subjects were examined, all the factors affecting LA functional properties could not be excluded.
8. Moreover, due to absence of dedicated software for LA segmentation, 3DSTE-derived LV segmentation model was used during analyses at the time of investigations.
9. One can argue about which atrium the atrial septum belongs to. In the present study it was considered to be an essential part of the LA.
10. 3DSTE could be performed only in subjects who are in sinus rhythm. If technical reasons do not prevent this, it would be worthwhile to compare the results with those of AF patients.
11. Ewing's SCRTs were used to examine the physiological responses to shifts in autonomic function affecting several factors including cardiac mechanics, hemodynamics, venous return, and afterload.[5]

5 | CONCLUSIONS

Significant correlations between features of vegetative autonomic function represented by Ewing's 5 SCRTs and specific LA functions represented by 3DSTE-derived LA volume-based functional properties and strains could be demonstrated in healthy adults.

CONFLICT OF INTEREST STATEMENT

The authors declare no conflicts of interest.

DATA AVAILABILITY STATEMENT

The data that support the findings of this study are available on request from the corresponding author. The data are not publicly available due to privacy or ethical restrictions.

REFERENCES

1. Seward JB, Hebl VB. Left atrial anatomy and physiology: echo/Doppler assessment. *Curr Opin Cardiol*. 2014;29:403-407.
2. Hoit BD. Left atrial size and function: role in prognosis. *J Am Coll Cardiol*. 2014;63:493-505.
3. Badano LP, Nour A, Muraru D. Left atrium as a dynamic three-dimensional entity: implications for echocardiographic assessment. *Rev Esp Cardiol*. 2013;66:1-4.
4. Nemes A, Forster T. Assessment of left atrial size and function – from M-mode to 3D speckle-tracking echocardiography. *Orv Hetil*. 2014; 155:1624-1631.
5. Ewing DJ, Martyn CN, Young RJ, Clarke BF. The value of cardiovascular autonomic function tests: 10 years experience in diabetes. *Diabetes Care*. 1985;8:491-498.
6. Netter F. *Atlas of Human Anatomy*. 6th ed. Elsevier Saunders; 2014.
7. Drake R, Vogl AW, Mitchell AWM. *Gray's Anatomy for Students*. 3rd ed. Churchill Livingston Elsevier; 2015.
8. Nemes A, Kalapos A, Domsik P, Forster T. Three-dimensional speckle-tracking echocardiography — a further step in non-invasive three-dimensional cardiac imaging. *Orv Hetil*. 2012;153:1570-1577.
9. Ammar KA, Paterick TE, Khanderia BK, et al. Myocardial mechanics: understanding and applying three-dimensional speckle tracking echocardiography in clinical practice. *Echocardiography*. 2012;29:861-872.
10. Urbano-Moral JA, Patel AR, Maron MS, Arias-Godinez JA, Pandian NG. Three-dimensional speckle-tracking echocardiography: methodological aspects and clinical potential. *Echocardiography*. 2012;29:997-1010.

10970096, 0, Downloaded from https://onlinelibrary.wiley.com/doi/10.1002/jcu.23603 by University Of Szeged, Wiley Online Library on [26/11/2023]. See the Terms and Conditions (https://onlinelibrary.wiley.com/terms-and-conditions) on Wiley Online Library for rules of use; OA articles are governed by the applicable Creative Commons License

11. Muraru D, Niero A, Rodriguez-Zanella H, Cherata D, Badano L. Three-dimensional speckle-tracking echocardiography: benefits and limitations of integrating myocardial mechanics with three-dimensional imaging. *Cardiovasc Diagn Ther*. 2018;8:101-117.
12. Lang RM, Badano LP, Mor-Avi V, et al. Recommendations for cardiac chamber quantification by echocardiography in adults: an update from the American Society of Echocardiography and the European Association of Cardiovascular Imaging. *Eur Heart J Cardiovasc Imaging*. 2015;16:233-270.
13. Nemes A, Kormányos Á, Domsik P, Kalapos A, Ambrus N, Lengyel C. Normal reference values of left atrial volumes and volume-based functional properties using three-dimensional speckle-tracking echocardiography in healthy adults (Insights from the MAGYAR-Healthy Study). *J Clin Ultrasound*. 2021;49:49-55.
14. Nemes A, Kormányos Á, Domsik P, Kalapos A, Lengyel C, Forster T. Normal reference values of three-dimensional speckle-tracking echocardiography-derived left atrial strain parameters (results from the MAGYAR-Healthy Study). *Int J Cardiovasc Imaging*. 2019;35:991-998.
15. Vágvölgyi A, Maróti Á, Szűcs M, et al. Peripheral and autonomic neuropathy status of young patients with type 1 diabetes mellitus at the time of transition from pediatric care to adult-oriented diabetes care. *Front Endocrinol (Lausanne)*. 2021;12:719953.
16. Ewing DJ, Clarke BF. Diagnosis and management of diabetic autonomic neuropathy. *Brit Med J (Clin Res Ed)*. 1982;285:916-918.
17. Nemes A, Kalapos A, Domsik P, Orosz A, Lengyel C. Correlations between left ventricular rotational mechanics and parasympathetic autonomic function – results from the three-dimensional speckle-tracking echocardiographic MAGYAR-Healthy Study. *Quant Imaging Med Surg*. 2021;11:1613-1618.
18. Nemes A, Takács R, Gavallér H, et al. Correlations between aortic stiffness and parasympathetic autonomic function in healthy volunteers. *Can J Physiol Pharmacol*. 2010;88:1166-1171.
19. Arora R, Ulphani JS, Villuendas R, et al. Neural substrate for atrial fibrillation: implications for targeted parasympathetic blockade in the posterior left atrium. *Am J Physiol Heart Circ Physiol*. 2008;294:H134-H144.
20. Xhaet O, de Roy L, Floria M, et al. Integrity of the ganglionated plexi is essential to parasympathetic innervation of the atrioventricular node by the right vagus nerve. *J Cardiovasc Electrophysiol*. 2017;28:432-437.

How to cite this article: Nemes A, Kormányos Á, Orosz A, Ambrus N, Várkonyi TT, Lengyel C. Correlations between vegetative autonomic function and specific left atrial functions in healthy adults: Insights from the three-dimensional speckle-tracking echocardiographic MAGYAR-Healthy Study. *J Clin Ultrasound*. 2023;1-8. doi:10.1002/jcu.23603

10970096, 0, Downloaded from https://onlinelibrary.wiley.com/doi/10.1002/jcu.23603 by University Of Szeged, Wiley Online Library on [26/11/2023]. See the Terms and Conditions (https://onlinelibrary.wiley.com/terms-and-conditions) on Wiley Online Library for rules of use; OA articles are governed by the applicable Creative Commons License